

Control of Tumor Initiation by NKG2D Naturally Expressed on Ovarian Cancer Cells^{1,2}



Xin Cai^{*,3}, Andrea Caballero-Benitez^{*,3}, Mesfin M. Gewe[†], Isaac C. Jenkins^{*}, Charles W. Drescher[‡], Roland K. Strong[†], Thomas Spies^{*} and Veronika Groh^{*}

^{*}Clinical Research Division, Fred Hutchinson Cancer Research Center, 1100 Fairview Ave. N., Seattle, WA, 98112, USA; [†]Basic Sciences Division, Fred Hutchinson Cancer Research Center, 1100 Fairview Ave. N., Seattle, WA, 98112, USA; [‡]Public Health Sciences Division, Fred Hutchinson Cancer Research Center, 1100 Fairview Ave. N., Seattle, WA, 98112, USA

Abstract

Cancer cells may co-opt the NKG2D lymphocyte receptor to complement the presence of its ligands for autonomous stimulation of oncogenic signaling. Previous studies raise the possibility that cancer cell NKG2D may induce high malignancy traits, but its full oncogenic impact is unknown. Using epithelial ovarian cancer as model setting, we show here that *ex vivo* NKG2D⁺ cancer cells have stem-like capacities, and provide formal *in vivo* evidence linking NKG2D stimulation with the development and maintenance of these functional states. NKG2D⁺ ovarian cancer cell populations harbor substantially greater capacities for self-renewing *in vitro* sphere formation and *in vivo* tumor initiation in immunodeficient (NOD scid gamma) mice than NKG2D⁻ controls. Sphere formation and tumor initiation are impaired by NKG2D silencing or ligand blockade using antibodies or a newly designed pan ligand-masking NKG2D multimer. In further support of pathophysiological significance, a prospective study of 47 high-grade serous ovarian cancer cases revealed that the odds of disease recurrence were significantly greater and median progression-free survival rates higher among patients with above and below median NKG2D⁺ cancer cell frequencies, respectively. Collectively, our results define cancer cell NKG2D as an important regulator of tumor initiation in ovarian cancer and presumably other malignancies and thus challenge current efforts in immunotherapy aimed at enhancing NKG2D function.

Neoplasia (2017) 19, 471–482

Introduction

The NKG2D lymphocyte receptor enables tumor immune surveillance by stimulating cytotoxic natural killer (NK) cells and CD8 T cells upon engagement of ligands that are induced on cancer cells [1]. However, progressing tumors in humans stifle immune responses by various tactics that include chronic stimulation and functional disabling of lymphocyte NKG2D. For example, in patients with advanced cancers, ligand engagement of NKG2D causes its down-modulation and degradation in NK cells and CD8 T cells [2]. Chronic engagement of NKG2D also affects unrelated CD3ζ-dependent lymphocyte receptor functions [3]. These negative effects are further escalated as cancer cells themselves may co-opt expression of NKG2D and thus complement the presence of its ligands for autonomous stimulation of oncogenic signaling [4]. In lymphocytes and cancer cells alike, stable NKG2D expression and function depend

Abbreviations: DAP10, DNAX-activating protein 10; EOC, epithelial ovarian cancer; HGS, high-grade serous; MICA and MICB, MHC class I-related chains A and B; NKG2DL, NKG2D ligands; ULBP, UL-16 binding protein

Address all correspondence to: Veronika Groh, MD, and Thomas Spies, PhD, Clinical Research Division, Fred Hutchinson Cancer Research Center, 1100 Fairview Ave. N., Seattle, WA 98109, USA.

E-mail: xcai@fredhutch.org

¹ Financial support: This work was supported by a Fred Hutchinson Cancer Research Center VIDD Faculty Initiative Award 2014 (R.K.S.) and NIH/NCI grant R01 CA174470 (T.S.).

² Disclosure of potential conflict of interest: No potential conflicts of interest were disclosed.

³ These authors contributed equally to this work.

Received 14 February 2017; Revised 20 March 2017; Accepted 24 March 2017

© 2017 The Authors. Published by Elsevier Inc. on behalf of Neoplasia Press, Inc. This is an open access article under the CC BY-NC-ND license (<http://creativecommons.org/licenses/by-nc-nd/4.0/>).

1476-5586

<http://dx.doi.org/10.1016/j.neo.2017.03.005>

on its association with the DNAX-activating protein 10 (DAP10) signaling adaptor, which initiates PI3K-AKT and mitogen-activated protein kinase signaling cascades [4,5]. In cancer cells, these pathways control various aspects of tumorigenesis [6,7]. NKG2D ligands (NKG2DL) include MHC class I-related chains A and B (MICA and MICB) and six members of the UL-16 binding protein (ULBP) family [8]. NKG2DL are typically absent from the surface of most normal cells but are induced by oncogenesis-associated cellular stress responses and other disease conditions [9]. NKG2DL are abundant in essentially all types of cancers but display variability in the representation of different ligand types [10,11].

In various types of cancers, the continuous presence of NKG2DL correlates with poor clinical outcomes [11–15]. One plausible explanation considers the role of NKG2DL in promoting tumor immune evasion [2,3]. An alternative possibility implicates oncogenic effects of cancer cell NKG2D lending selective advantage to NKG2DL expression [4]. NKG2D may have the capacity to promote cancer cell plasticity and stemness reprogramming, cellular changes that are considered central to tumor dissemination and metastasis formation [16]. This notion is supported by a study of a cohort of breast, ovarian, colon, and prostate cancers showing that frequencies of NKG2D-positive cancer cells positively correlate with tumor stage, and by the presence of high-plasticity markers in NKG2D-positive model tumor lines and *ex vivo* breast cancer cells [4,17]. As of yet, however, functional *in vivo* evidence that cancer cell NKG2D may impart *bona fide* stem-like attributes is missing. Moreover, current clinical evidence for pathophysiological significance is insufficient due to previous inclusion of heterogeneous cancer cases [4]. This report aims at closing these knowledge gaps using epithelial ovarian cancer (EOC) as a model setting. EOCs typically express abundant NKG2DL, which are strongly associated with negative disease outcomes [11,13]. Oncogenic effects of cancer cell NKG2D could thus be particularly apparent in this malignancy.

We report here that cancer cell NKG2D has negative clinical effects in a prospective analysis of high-grade serous (HGS) ovarian cancer, and present *in vitro* experiments and mouse model xenograft assays providing evidence that links NKG2D signaling to induction of cancer stem cell attributes and tumor initiation.

Materials and Methods

Ex Vivo and Xenograft Ovarian Cancer Specimens, Cell Suspensions, and Cell Lines

Primary EOC surgical specimens and annotated histopathology, International Federation of Gynecologists and Obstetricians (FIGO) tumor stage, and patient follow-up information were obtained from the Cooperative Human Tissue Network (www.chtn.nci.nih.gov) and the Pacific Ovarian Cancer Research Consortium Specimen Repository under Fred Hutchinson Institutional Review Board protocol #6007/552. Xenograft-derived tumors were harvested in accordance with Fred Hutchinson Institutional Animal Care and Use Committee protocol #1870. Processing of tumor specimens to single cell suspensions used a Human Tumor Tissue Dissociation Kit and a gentleMACS Dissociator (both Miltenyi Biotech). Single-cell processing of tumor spheres was in phosphate-buffered saline (PBS) with 2 mM EDTA. The MDAH-2774 tumor line (American Type Culture Collection) was grown in RPMI-1640/10% fetal bovine serum. Cells were used within 25 passages not exceeding a period of 3 to 4 months of revival. The American Type Culture Collection uses

Table 1. Grouping of the 47 EOC Study Cases Based on NKG2D Positivity, and Summary of Clinical Parameters

Parameter	Total (N = 47)	NKG2D Low (n = 24)	NKG2D High (n = 23)
% NKG2D ⁺ cells (median, min-max)	1.79 (0.00-66.90)	0.93 (0.00-1.79)	12.87 (2.18-66.90)
Age (median, lowest-highest)	61 (38-82)	62 (38-82)	59 (44-77)
FIGO stage (n, %)			
I/II	9 (19)	6 (25)	3 (13)
III/IV	38 (81)	18 (75)	20 (87)
Outcome (n, %)			
ANED	27 (57)	19 (79)	8 (35)
Recurrence	14 (30)	3 (13)	11 (48)
DOD	6 (13)	2 (8)	4 (17)

ANED, alive, no evidence of disease; DOD, died of disease.

morphological, cytogenetic, and DNA profile analysis for authentication. The cytotoxic NKL cell line (gifted from Drs. Robertson and Ritz, Dana Farber Cancer Institute [18]) was grown in RPMI-1640/10% human serum/interleukin 2 (100 IU; Chiron).

Clinical Association Study

A total of 47 primary EOC cases (surgical specimens procured between January 2009 and June 2015) were included into the study. All tumors represented HGS carcinoma [19]. FIGO stage and disease outcome annotations are summarized in Table 1. Patient treatments uniformly involved primary surgery followed by chemotherapy. Postoperative follow-up periods varied.

Transfectants and siRNA Transduction

MDAH-2774–derived NKG2D-DAP10 transfectants (MDAH-2774-TF cells) have been described [17]. Additional transfectants with vector control (MDAH-2774 mock cells) and NKG2D RNAi (MDAH-2774-TF-KO)– or scrambled RNAi–transduced lines (MDAH-2774-TF-scrRNAi) were generated as described [4]. Depletion of NKG2D in MDAH-2774-TF-KO cells has been confirmed as described ([4,17]; see Supplementary Figure S1). C1R-MICA, C1R-MICB, EL4-ULBP1, EL4-ULBP2, EL4-ULBP3, Mel-ULBP4, EL4-ULBP5, and C1R-ULBP6 transfectants have been described [20]. Silencing of NKG2D in *ex vivo* ovarian cancer cells was as with the MDAH-2774-TF line.

Engineering a Biologic Inhibitor of NKG2D Signaling

“Single-chain dimer” forms of NKG2D (NKG2D^{scd}) were designed using a segment of the N-terminal arm of NKG2D as a linker between domains within the native homodimer. NKG2D^{scd} targeting units were multimerized through fusion with the minimal heptamerization motif from human C4b binding protein (C4bbp) [21], yielding highly avid NKG2D^{scd} heptamers (NKG2D^{scd}₇). Both NKG2D^{scd} and NKG2D^{scd}₇ proteins were expressed using the Daedalus platform in HEK293F cells (Invitrogen) as fusions with Siderocalin (Scn) to stabilize expression [22,23]. A Tobacco Etch Virus protease [24] scission site (EDLYFQ) was inserted between the Scn and NKG2D moieties, and N-terminal polyhistidine and FLAG (DYKDDDDK) tags were incorporated to facilitate purification. Recombinant proteins were purified from culture supernatants by immobilized metal chelate affinity, treated with Tobacco Etch Virus protease to release the Scn fusion partner, and polished by size exclusion chromatography (SEC). Purity and proper folding were confirmed by comparative reduced/nonreduced sodium dodecyl sulfate polyacrylamide gel electrophoresis and analytical SEC.

Endotoxin levels were checked using the PyroGene rFc assay (Lonza), and NKG2D^{scd}₇ was labeled with fluorescein isothiocyanate (Sigma-Aldrich) at a ratio of two fluorophores per protomer.

Surface plasmon resonance (SPR) interaction analyses confirming that NKG2D^{scd} and NKG2D^{scd}₇ retain proper binding to NKG2DL were performed at 25°C with Biacore T100 instrumentation on a Series S CM5 chip (GE Healthcare). NKG2D^{scd} and NKG2D^{scd}₇ proteins were immobilized using standard amine coupling chemistry, yielding surfaces with ~310 or ~240 SPR response units, respectively. A reference surface was generated by activating and deactivating a flow cell in the absence of protein. Serial two-fold dilutions of soluble, wild-type MICA (240 nM to 0.47 nM, or 100 nM to 0.78 nM), produced as previously described [25], were prepared in a running buffer of HBS-EP+ (10 mM HEPES, pH 7.4, 150 mM NaCl, 3 mM EDTA, 0.05% surfactant P-20; GE Healthcare) with 0.1 mg/ml bovine serum albumin. Duplicate MICA samples, interspersed with multiple buffer blanks, were randomly injected at 50 µl/min, with 3 minutes of association and 5 minutes of dissociation. Surfaces were regenerated with a 10-second injection of 10 mM glycine, pH 2.0, followed by 2 minutes of buffer stabilization. Double-referenced data were fit with a 1:1 binding model using BIAevaluation 2.0.4 software (GE Healthcare).

Sphere Formation Assay

Tumor cells were cultured at 5×10^3 , 1×10^4 , and 5×10^4 cells/ml when using *ex vivo* cancer cells, or 1×10^3 cells/ml when using tumor lines, in 96-well ultra-low-attachment plates in mammary epithelial cell growth medium (Lonza) with 0.9% methylcellulose (Sigma Aldrich). After 3 to 4 weeks, >100 µm-diameter tumor spheres were microscopically counted in triplicate wells. For serial passaging, primary spheres were dissociated to single cells and replated in mammary epithelial cell growth medium. Cultures were monitored for secondary and tertiary sphere formation for up to 4 weeks. To block NKG2D-NKG2DL engagement, assays were in the presence of either a cocktail of antibodies (Abs) specific for MICA/B (6D4; BD Pharmingen) and ULBP1-6 [clones 170,818 (ULBP1), 165,903 (ULBP2,5,6), and 166,510 (ULBP3) from R&D Systems and clone 1H11 (ULBP4; 20)], each at 10 µg/ml, or control isotype immunoglobulin (Ig), or the pan-NKG2DL-binding NKG2D^{scd}₇ (10 µg/ml) or PBS control. Agonist anti-NKG2D Ab (clone 149,810) was from R&D Systems [26].

Animal Studies

All animal procedures were approved by Fred Hutchinson Institutional Animal Care and Use Committee protocol #1870. Female nonobese diabetic/severe combined immunodeficient (NOD/SCID) and NOD scid gamma (NSG) mice (6-8 weeks old) were obtained from the Fred Hutchinson Core Center of Excellence in Hematology (DK-56465 and DK-106829) and housed under pathogen-free conditions at the institutional Comparative Medicine Shared Resource. For implants, mice were anesthetized with isoflurane and injected subcutaneously into dorsal flanks with either *ex vivo* isolated cancer cells or MDAH-2774-derived lines, each in 100-µl growth medium (1:1 PBS/BD Matrigel Matrix; BD Bioscience). Tumor development was monitored three times per week until tumor nodules were palpable and then in daily intervals. At experimental end points or when a tumor parameter reached 1.5 cm, animals were euthanized and tumors resected. For *in vivo* NKG2DL masking, mice were treated in weekly intervals (up to 4 weeks

posttransplant) with either a cocktail of anti-MICA/B and anti-ULBP1, -ULBP3, -ULBP4, and -ULBP5 Abs (see above) or NKG2D^{scd}₇ or relevant controls, all administered subcutaneously at the site of tumor cell implants or *via* tail vein injection. Antibody or NKG2D^{scd}₇ dosages were 10 µg per local application or 100 µg per tail vein injection.

Flow Cytometry and Fluorescence Microscopy

Ex vivo EOC- or xenograft tumor-derived cell suspensions or sphere-derived single cells (in PBS/10% human serum/0.15% sodium azide) were variably incubated with pretitrated Ab-fluorochrome conjugates to NKG2D (clone 1D11; APC), CD45 (clone 2D1; APC-H7), CD44 (clone G44-26; PerCP-Cy5.5) (all BD Pharmingen), and EpCAM (clone 9C4; Alexa Fluor 488; Biolegend). NKG2DL expression was examined using an Ab cocktail (see above). Anti-H2Dd (clone 34-2-12; Biolegend) was used for exclusion of murine cells. DAPI was used for live/dead cell distinction. Isotype Igs were used as controls, and background fluorescence was subtracted. For the clinical association study, cancer cells were defined as CD45⁻EpCAM⁺. Because EpCAM expression levels can vary substantially among cancer cells [27], all nonhematopoietic (CD45⁻) cells with above threshold EpCAM staining were scored. Testing for tumor cell aldehyde dehydrogenase activity was with the ALDEFLUOR kit (Stemcell Technologies) according to the manufacturer's instructions. Briefly, tumor cells were incubated with ALDEFLUOR {boron, [N-(2,2-diethoxyethyl)-5[(3,5-dimethyl-2H-pyrrol-2-ylidene-kN)methyl]-1H-pyrrole-2-propanamida to KN1] difluoro-, (T-4)-(9CI)} in the absence or presence of ALDH1 activity inhibitor diethylaminobenzaldehyde (DEAB) for 30 minutes at 37°C followed by one wash using ALDEFLUOR assay buffer (Stemcell Technologies) and surface staining for NKG2D, CD45, and EpCAM. DEAB-treated cells served to set baseline ALDH1 activities. To confirm binding of NKG2D^{scd}₇ to all NKG2DL, corresponding transfectants (see above) were incubated with FITC-conjugated NKG2D^{scd}₇ (2 µg/ml) or PBS control for 30 minutes on ice followed by two PBS washes. Stained cells were analyzed using a BD LSRII flow cytometer (BD Biosciences) and FlowJo software (Tree Star). Cell sorting was on a FACS Aria (BD Biosciences). To visualize binding of NKG2D^{scd}₇ to MICA at the cell surface, HEK293F cells were transiently transfected with a MICA-eGFP fusion protein, cultured for 24 hours, and subsequently incubated for 1 hour at 37°C with 1 µmol of Cy5.5-labeled NKG2D^{scd}₇. Fluorescence imaging was with an EVOS microscope (Thermo Fisher Scientific). Cy5.5 labeling of NKG2D^{scd}₇ was with Cy5.5 NHS ester (GE Health Care Life Sciences) at a fluorophore:protomer ratio of 0.5 using the manufacturer's recommended protocol.

Cytotoxicity Assay

CellTrace Violet (Life Technologies)-labeled C1R-MICA and Oregon Green^R 488 (ThermoFisher Scientific)-labeled C1R-mock target cells were mixed at equal numbers and exposed to NK cells at 1:1 effector to target ratios in the presence or absence of NKG2D^{scd}₇ (10 µg/ml) or PBS control. Anti-MICA/B Ab 6D4 (10 µg/ml) served as positive blocking control. Following 4-hour incubation at 37°C, effector/target cell mixes were stained using LIVE/DEAD Fixable Aqua Dead Cell Stain Kit (Molecular Probes) and analyzed by flow cytometry. Ratios of live C1R-mock to C1R-MICA cells were used as measure of cytotoxic activity.

Statistical Analyses

Frequencies of NKG2D-positive (from here on noted as NKG2D⁺) cancer cells were divided into subgroups represented by

NKG2D Low (\leq median % NKG2D⁺ cells) and NKG2D High ($>$ median % NKG2D⁺ cells). Logistic regression models were used to characterize the relationship between NKG2D subgroups and clinical parameters. More specifically, we modeled the probability of disease recurrence or high tumor stage (I/II vs III/IV) among the subgroups while adjusting for patient age. In addition, a proportional hazards model was used to examine the hazard of progression or death among NKG2D subgroups while adjusting for patient age and tumor stage. Model results are reported in terms of odds (ORs) or hazard (HRs) ratios, with the NKG2D Low subgroup as reference category. All model *P* values were derived from likelihood ratio statistics and are two-sided. No other covariates were available for inclusion in the models. Kaplan-Meier curves and the log-rank test were used to analyze progression-free survival rates between the subgroups. All analyses were performed using R version 3.3.1 [28]. Extreme Limiting Dilution Analysis (ELDA) was as described [29].

Results

Relationship between NKG2D-Positive Cancer Cells and Negative Disease Outcomes in Epithelial Ovarian Cancer

We previously determined that cell surface flow cytometry of *ex vivo* isolated tumor cells is the method of choice for enumerating cancer cells expressing signaling competent NKG2D [4]. HGS EOC specimens were thus examined by flow cytometry for frequencies of cancer cells positive for surface NKG2D. Consistent with previous findings, NKG2D⁺ cancer cells were present in all but one of the EOC specimens with frequencies between 0.1% and 66.9% (median 1.79%; Table 1; 4). No NKG2D positivity was recorded among CD45⁻EpCAM⁻ cells. For statistical appraisal of relationships between frequencies of NKG2D⁺ cancer cells and clinical parameters, the cases studied were split into subgroups represented by NKG2D Low (\leq median % NKG2D⁺ cells) and NKG2D High ($>$ median % NKG2D⁺ cells) (Table 1). As per likelihood ratio test, the odds of disease recurrence were significantly greater for the NKG2D High subgroup [OR = 12.4; 95% confidence interval (CI) = 3.0, 70.3; *P* < .001; Figure 1A and Supplementary Table S1]. Moreover, median progression-free survival rates were lower among the NKG2D High subgroup cases (1.8 vs 6+ years; *P* = .063; Figure 1B). When adjusted for age and tumor stage, these cases demonstrated an increased, albeit nonsignificant, risk of progression or death (HR = 1.9; 95% CI = 0.7, 5.5; *P* = .20). Lastly, the NKG2D High subgroup, though not significant, tended to have higher tumor stages (FIGO III/IV) than the NKG2D Low subgroup (OR = 2.1; 95% CI = 0.5, 11.1; *P* = .35; Figure 1C). Altogether, these results implied negative clinical effects of cancer cell NKG2D.

Association of NKG2D with Markers of Cellular Plasticity among Ex Vivo Ovarian Cancer Cells

With breast cancer cells, expression of NKG2D preferentially segregates with marker profiles characteristic of the epithelial-mesenchymal transition and metastable capacities [17]. To test whether similar relationships apply to HGS EOC, *ex vivo* isolated tumor cell suspensions were examined by flow cytometry for nonhematopoietic (CD45⁻) NKG2D and markers of high-plasticity traits represented by EpCAM together with CD44, or high aldehyde dehydrogenase (ALDH1) enzymatic activity [30–32]. In a first set of five tumor specimens (EOC1 through EOC5; see Supplementary Table S2 for clinical parameters of EOC specimens used throughout the remainder of study), proportions of EpCAM⁺CD44⁺ cells were larger among NKG2D⁺ as compared to NKG2D⁻ cell populations

[33.5% (\pm 36.2) vs 3.5% (\pm 3.3); Supplementary Table S3]. A second set of seven CD45⁻ tumor cell suspensions was examined for NKG2D and ALDH1 activity, which is considered the most stringent readout for high cancer cell plasticity and was determined by ALDEFLUOR substrate conversion assay. All samples showed substantial overlaps between expression of NKG2D and ALDH1 activity, with a mean proportion of 30.2% (\pm 19.4) of NKG2D⁺ cells scoring high for ALDH1 activity and most ALDEFLUOR^{high} cells staining positive for NKG2D (Figure 2, A and B; Supplementary Table S3). EOC is a heterogeneous disease commonly classified by histology and grade as type I or type II (predominantly HGS) [19]. Analysis by flow cytometry of three type I EOC specimens recapitulated the findings obtained earlier with the panel of HGS EOCs, suggesting EOC subtype independence (Supplementary Table S3). Hence, we conclude that EOC cell populations with surface NKG2D are enriched for cells with phenotypic attributes that have been associated with high cellular plasticity and stem cell-like functions.

In Vitro Evidence for Stem Cell-Like Sphere-Formation Capacities of NKG2D⁺ Ovarian Cancer Cells

Stem cell-like cancer cells have the ability to form tumor spheres in cell culture [33–35]. We FACS Aria sorted CD45⁻NKG2D⁺ and control NKG2D⁻ cancer cells from altogether eight *ex vivo* HGS EOC tumor cell suspensions. Cells were cultured under classical adherence-independent sphere-formation conditions and monitored for the appearance of spheres over a 3-week period. NKG2D⁺ cells from all tumors formed numerous large ($>$ 100 μ m diameter) spheres even when plated at low cell densities, whereas control NKG2D⁻ cells generated spheres only when plated at high density and those that developed were rare and typically small (Figure 3, A and B). NKG2D expression in spheres derived from NKG2D⁺ cells was monitored by flow cytometry of single cell-dissociated spheres. Although most cells stably retained NKG2D, some were negative, suggesting that NKG2D⁺ cells may be able to give rise to NKG2D⁻ cells (Figure 3C). Spheres derived from NKG2D⁻ cells remained NKG2D negative (Supplementary Figure S2A). Cancer cells usually express diverse combinations of NKG2DL that vary between tumors and individual cells [10,11,13]. Presence of NKG2DL on sphere cells, a prerequisite for NKG2D signaling, was confirmed using a cocktail of Abs to all NKG2DL (MICA/B and ULBP1 through ULBP6; Figure 3C). To test for self-renewal capacity of sphere-forming cells, primary spheres derived from NKG2D⁺ or control NKG2D⁻ cells (from specimens EOC22 and EOC23; Figure 3B) were dissociated, and equal cell numbers were plated for examination of secondary and tertiary sphere formation. Consistent with a relationship between NKG2D expression and stem cell-like attributes, only spheres originating from NKG2D⁺ cells could be passaged (Figure 3B [33]).

In support of a causal involvement of NKG2D in sphere formation, the sphere-forming abilities of NKG2D⁺ cancer cells were significantly reduced when NKG2D was depleted by recombinant lentivirus-mediated RNAi targeting, whereas control scrambled RNAi had no effect (Figure 3D). Similarly, culture of NKG2D⁺ cancer cells in the presence of anti-NKG2DL Abs diminished their sphere-formation capacity (Figure 3E), thus confirming that NKG2D signaling triggered by ligand engagement underlies the observed effect. Conversely, exposure of NKG2D⁺ cancer cells to an agonist anti-NKG2D antibody enhanced sphere formation (Figure 3E). As with type II EOC, sphere formation of type I EOC-derived NKG2D⁺ cancer cells also exceeded that of their NKG2D⁻ counterpart (Supplementary Figure S2B).

In Vivo Evidence for Stem Cell-Like Tumor-Initiating Capacities of NKG2D⁺ Ovarian Cancer Cells

Experimental proof of stem cell-like functions requires documentation of efficient tumor-initiating capacities upon xenografting in immunodeficient mice [36]. FACSARIA-sorted CD45⁻NKG2D⁺ or control NKG2D⁻ cells from two HGS EOC tumor cell suspensions

were subcutaneously inoculated at dosages of 5×10^3 and 1×10^4 cells into flanks of NSG mice. Three out of seven 5×10^3 and six out of eight 1×10^4 NKG2D⁺ cell implants initiated tumors as early as 6 weeks postinoculation. In contrast, only one of eight 1×10^4 NKG2D⁻ cell implants led to tumor formation 14 weeks postinoculation (Figure 3F). ELDA is commonly used for computational comparisons of enriched and depleted populations in stem cell assays [29]. Application of ELDA-based calculations revealed significant differences in the frequencies of cells with tumor-initiating abilities among NKG2D⁺ as opposed to NKG2D⁻ populations (Figure 3F). Similar differences in tumor-initiating capacities were recorded with NKG2D⁺ and NKG2D⁻ cells isolated from a type 1 EOC specimen (EOC36) (Figure 3F). Flow cytometry of NKG2D⁺ implant-derived xenografts confirmed that NKG2D and NKG2DL were stably maintained on most tumor cells (Figure 3G). However, as with the *in vitro* tumor sphere cultures, xenografts contained cells that lacked NKG2D, suggesting that NKG2D⁺ cells can give rise to NKG2D⁻ cells (Figure 3G). Tumors derived from NKG2D⁻ cells remained NKG2D negative (Supplementary Figure S2C). Altogether, these data suggest that NKG2D⁺ ovarian cancer cell populations are enriched for cells with stem cell-like tumor-initiating abilities.

NKG2D Stimulates Cancer Stem Cell-Like Tumor Initiation

Direct involvement of NKG2D in tumor initiation was initially explored using experimental variants and controls of the MDAH-2774 ovarian tumor line which lacks endogenous NKG2D [17]. Cells transfected with signaling-competent NKG2D-DAP10 (MDAH-2774-TF) or vector control (MDAH-2774 mock), or transduced with NKG2D RNAi (MDAH-2774-TF-KO) or scrambled RNAi control (MDAH-2774-TF-scrRNAi) have been previously established [17] or were newly made. MDAH-2774-TF cells recapitulated sphere formation as recorded with *ex vivo* NKG2D⁺ ovarian cancer cells (Figure 4, A and B) and were thus considered suitable for *in vivo* tumor initiation experiments in NOD/SCID mice.

In limiting dilution xenograft assays, three of four implants of as few as 100 MDAH-2774-TF cells formed tumors. Saturating tumor take with untransfected or mock transfected MDAH-2774 cells required implants of 1×10^4 cells (Figure 4C). NKG2D depletion in MDAH-2774-TF-KO cells restored negative control tumor formation rates (Figure 4C). Involvement of NKG2D signaling by ligand engagement was formally confirmed by grafting mice with saturating (1×10^4) or limiting (1×10^2) MDAH-2774-TF cell numbers and administration of NKG2DL Abs (see Supplementary Figure S3 for expression of NKG2DL). Ab administration, either at the cell

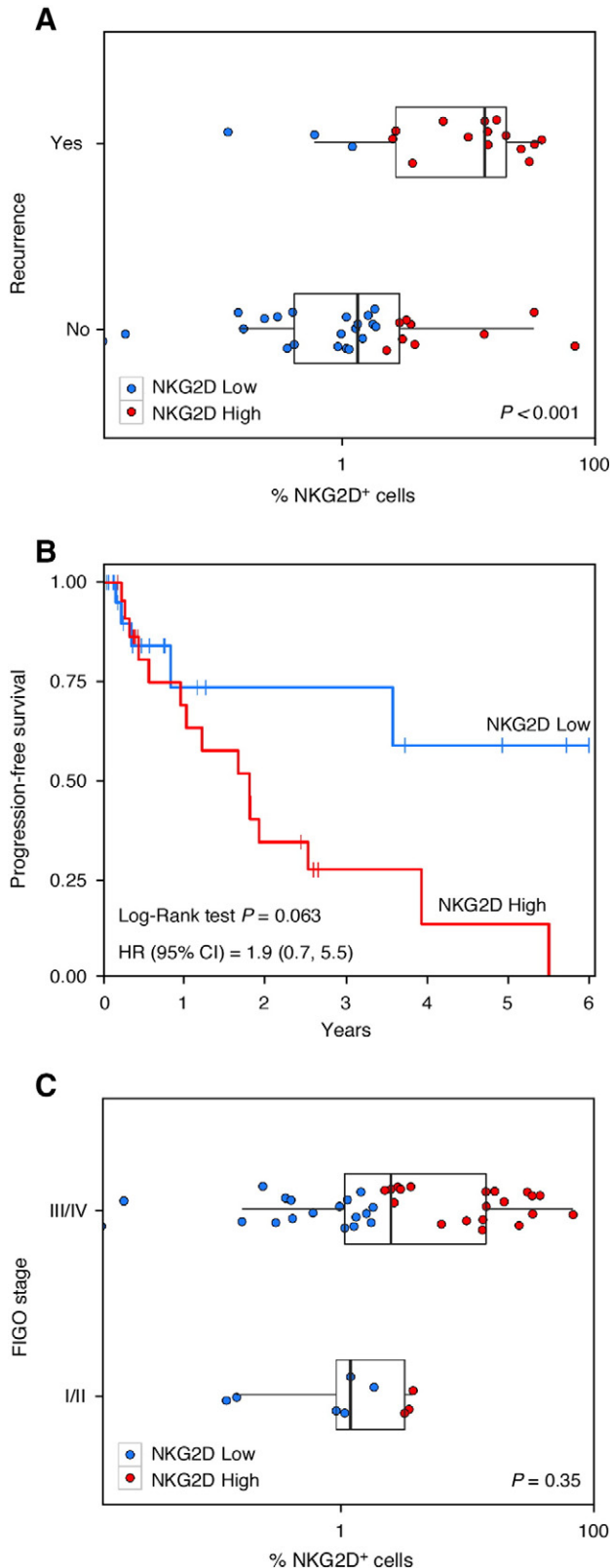


Figure 1. Negative clinical effects of cancer cell NKG2D in HGS EOC patients. (A) Box and whisker plots in graph depict % NKG2D⁺ cancer cells in patients with (yes) and without (no) disease recurrence. Vertical lines in boxes represent quartiles. Whiskers extend to the furthest value within 1.5 times the inner quartile range. Each dot represents one patient's % NKG2D⁺ value; the distribution along the Y-axis is randomized for visualization. Dots are colored by NKG2D⁺ subgroup, and those beyond the whiskers are considered outliers. The P value results from likelihood ratio test. (B) Kaplan-Meier curve comparing progression-free survival of patients in the NKG2D Low (blue line) and NKG2D High (red line) groups. The P value for the difference between NKG2D subgroups was determined by the log-rank test. HR results from a proportional hazards model and is adjusted by patient age and tumor stage. (C) Box and whisker plots depicting % NKG2D⁺ cancer cells in patients grouped based on FIGO stage. The P value results from likelihood ratio test.

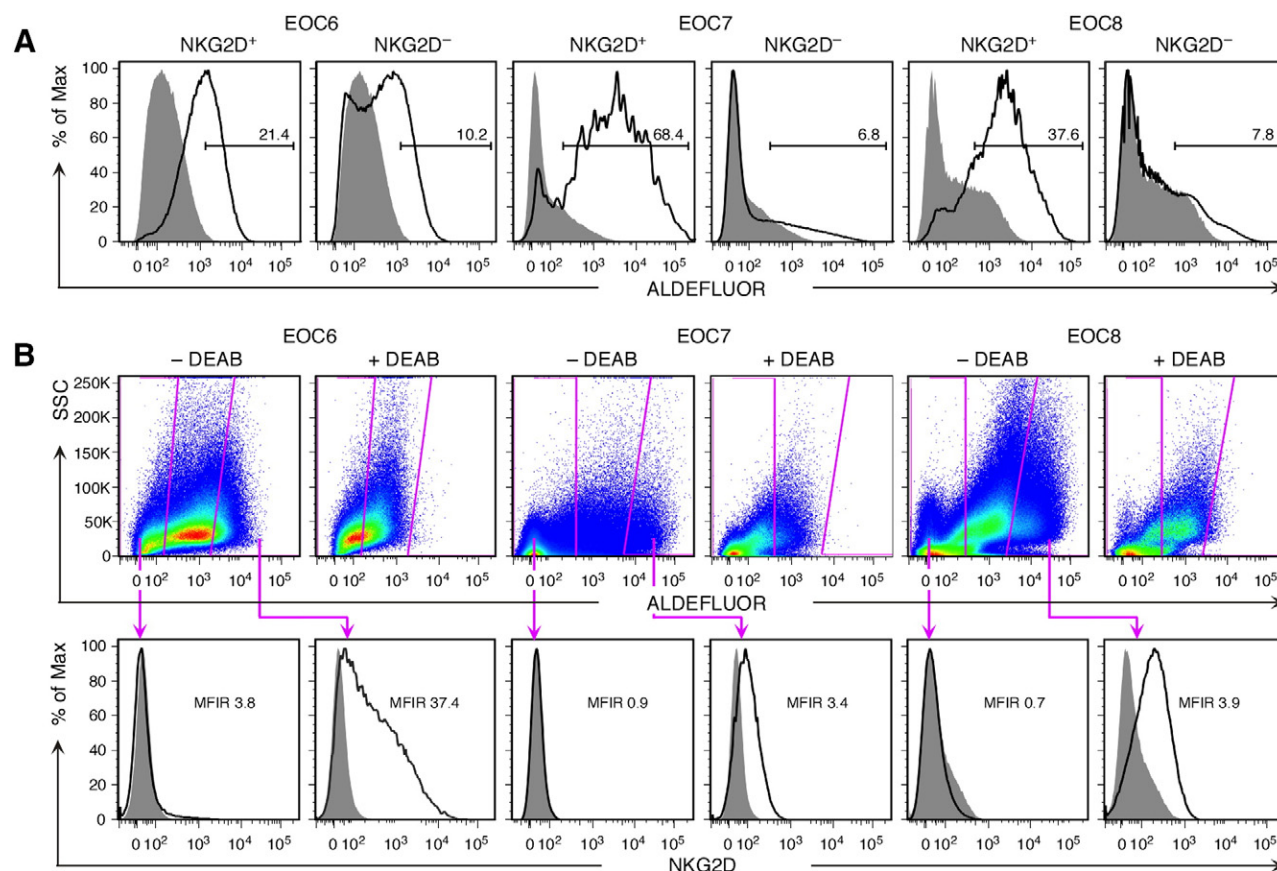


Figure 2. Association of NKG2D with high ALDH1 activity in *ex vivo* HGS EOC cells as measured by ALDEFLUOR substrate conversion. (A) Examples (EOC6, EOC7, and EOC8) of flow cytometry histogram pairs displaying ALDEFLUOR fluorescence profiles of CD45⁻NKG2D⁺ or NKG2D⁻ cancer cells. Open and filled gray profiles show ALDH1 activity in the absence and presence of the ALDH1 inhibitor DEAB, respectively. Numbers above bars represent % cells scoring high for ALDH1 activity. (B) Flow cytometry dot plots depict gates, and histograms below show corresponding NKG2D expression profiles of ALDEFLUOR^{high} and ALDEFLUOR^{low} cancer cells. Boxed gates in upper dot plots represent cells with high ALDH1 activity (at right) and cells certain to lack ALDH1 activity (at left). Dot plots of DEAB (+DEAB)-treated cell samples serve to set background ALDH1 activity. Open and filled gray histogram profiles display NKG2D and isotype Ig control staining, respectively. Numbers in histograms indicate mean fluorescence intensity ratios (MFIR). Data shown are representative of seven HGS EOC specimens (EOC6 through EOC12).

inoculation site or *via* tail vein injections, enhanced latency and reduced or prevented tumor formation (Figure 4D).

To reinforce significance of these cell line-based experiments, we examined tumor initiation by *ex vivo* NKG2D⁺ ovarian cancer cells sorted from HGS EOC37 (see Supplementary Table S2) and transduced with NKG2D RNAi or control scrRNAi. None of four 1.5×10^4 cell implants of NKG2D-silenced cells led to tumor formation in NSG mice, whereas three of four control cell inoculations generated tumors. Altogether, these results establish a link between NKG2D and the tumor-initiating potential residing within NKG2D⁺ ovarian cancer cell populations.

Blockade of Tumor Initiation By Pan Ligand-Reactive NKG2D-Based Multimer

Cancers express diverse combinations of NKG2DL with variability between tumors [10,11,13]. Confirmation of NKG2DL involvement in NKG2D-driven tumor initiation thus required an all-inclusive ligand masking approach. With pan-reactive Abs unavailable, we developed a soluble form of NKG2D suitable for global ligand binding (Figure 5; Supplementary Figure S4A). To stabilize folding, the native NKG2D homodimer was reengineered as a single-chain unit, analogous to an Ab single-chain Fv construct (Figure 5, A–C).

To enable tight binding, avidity was seven-fold increased by fusing a multimerization domain to the single-chain NKG2D binding module (Figure 5, C and D). Solution biochemistry ascertained proper folding of the heptamerized single-chain reagent (NKG2D^{scd7}; Figure 5, E and F). Functionality of NKG2D^{scd7} was initially confirmed by SPR binding analyses (Supplementary Figure S4B). Colocalization of NKG2D^{scd7} and MICA on the cell surface was visualized by fluorescence microscopy using Cy5.5 NHS ester-labeled NKG2D^{scd7} and HEK293F cells transfected with a MICA-eGFP fusion protein (Supplementary Figure S5A). Binding of NKG2D^{scd7} to all human NKG2DL was confirmed using individual transfectants and flow cytometry (Supplementary Figure S5B). Moreover, in a cytotoxicity assay, NKG2D^{scd7} but not solvent control interfered with lysis of NKG2DL-expressing target cells by the NKG2D⁺ NKL NK cell line (Supplementary Figure S5C; [37]). In sphere-forming assays, NKG2D^{scd7} inhibited sphere formation by *ex vivo* NKG2D⁺ ovarian cancer or MDAH-2774-TF cells (Figure 6, A and B).

Thereafter, NKG2D^{scd7} was used for testing of an involvement of NKG2DL in tumor initiation by *ex vivo* NKG2D⁺ ovarian cancer cells. Administrations (either locally at cell inoculation sites or systemically) prevented or reduced tumor formation, thus formally linking NKG2DL engagement and NKG2D stimulation to the

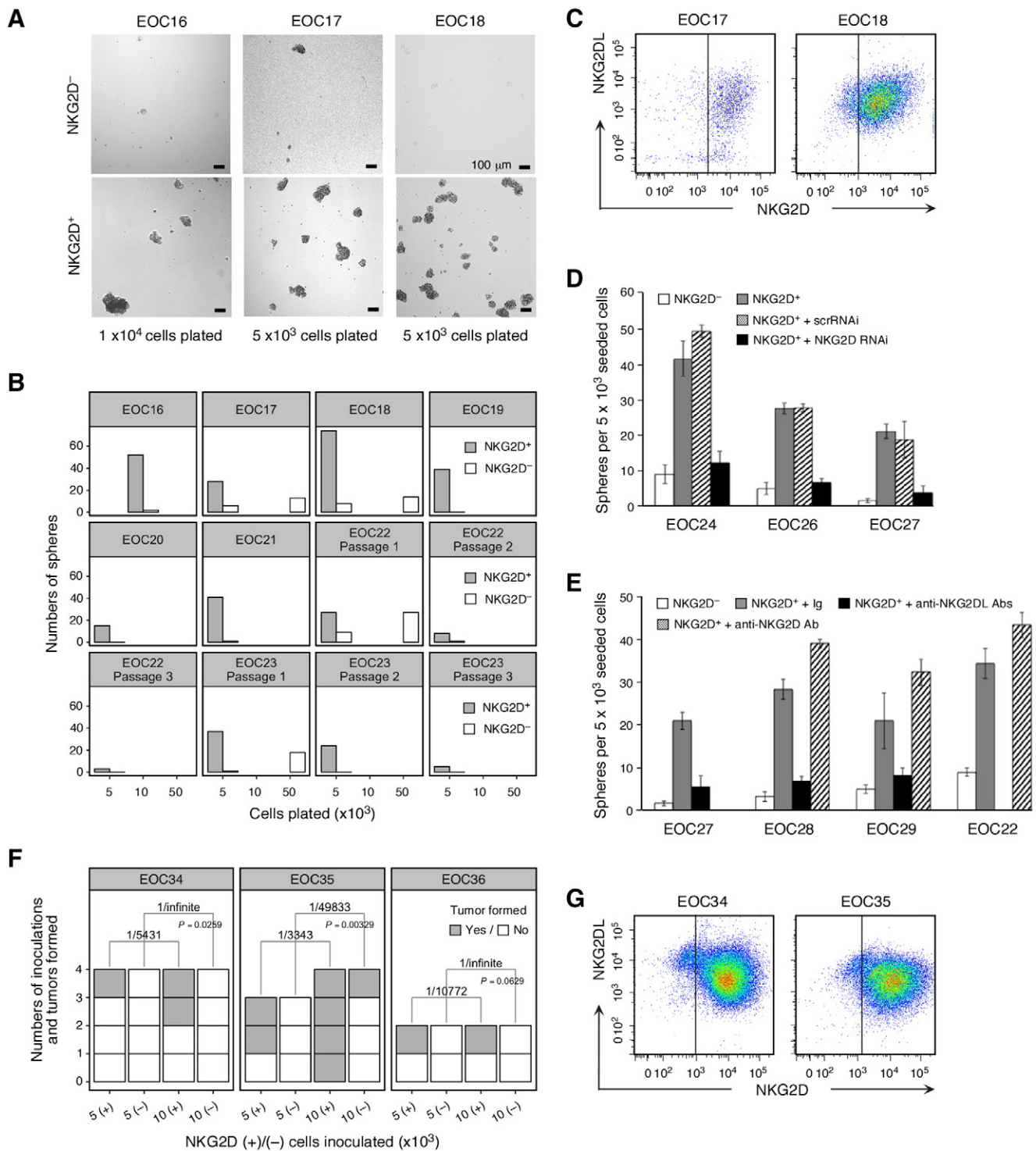
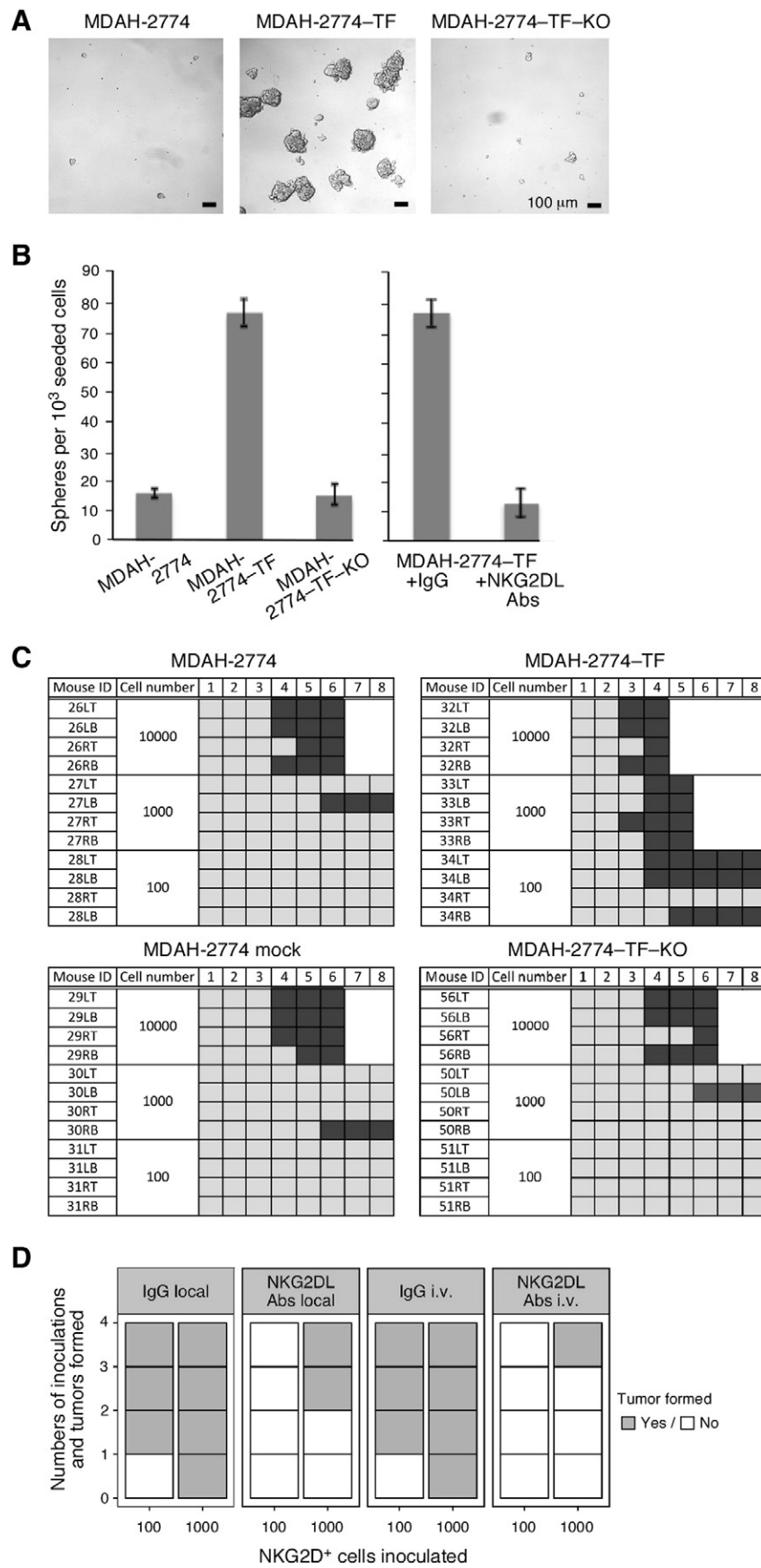


Figure 3. Tumor sphere formation and tumor initiation by *ex vivo* NKG2D⁺ HGS EOC cells. (A) Phase contrast micrographs of tumor spheres formed by NKG2D⁺ or NKG2D⁻ cancer cells FACSria-sorted from EOC16, EOC17, and EOC18 specimens. Cell numbers plated are indicated below each micrograph pair. (B) Display of sphere (>100 μm) numbers formed by NKG2D⁺ or NKG2D⁻ cancer cells from specimens EOC16 through EOC23 (serial passages for EOC22 and EOC23) and plated at the indicated cell numbers. Specimen size limitations precluded plating of all cell concentrations per EOC sample. (C) Flow cytometry dot plots showing NKG2D and NKG2DL expression on single cells dispersed from spheres formed by NKG2D⁺ cancer cells. Vertical lines separate positive from negative NKG2D staining and are drawn based on isotype Ig fluorescence. (D and E) Bar graphs displaying average numbers (from triplicate wells seeded with 5 × 10³ cells) of spheres (>100 μm) formed by NKG2D⁺ cancer cells (D) untreated (gray bars) or transduced with NKG2D RNAi (black bars) or control scrRNAi (hatched bars), and (E) in the presence of control isotype Ig (gray bars), anti-NKG2DL Abs (black bars), or anti-NKG2D Ab (hatched bars). Open bars represent average numbers of spheres formed by NKG2D⁻ cancer cells. (F) Xenograft tumor incidence expressed as numbers of tumors developed per number of inoculations of 5 or 10 × 10³ *ex vivo* NKG2D⁺ or NKG2D⁻ cancer cells into NSG mice. Frequencies of tumor initiating cells (numbers above brackets) and P values were computed using ELDA. EOC34 and EOC35 are HGS EOC cases; EOC36 represents a type I EOC. (G) Flow cytometry dot plots of NKG2D and NKG2DL expression on single cells isolated from xenograft tumors derived from NKG2D⁺ cancer cells. Vertical lines separate positive from negative NKG2D staining and are drawn based on isotype Ig background fluorescence.



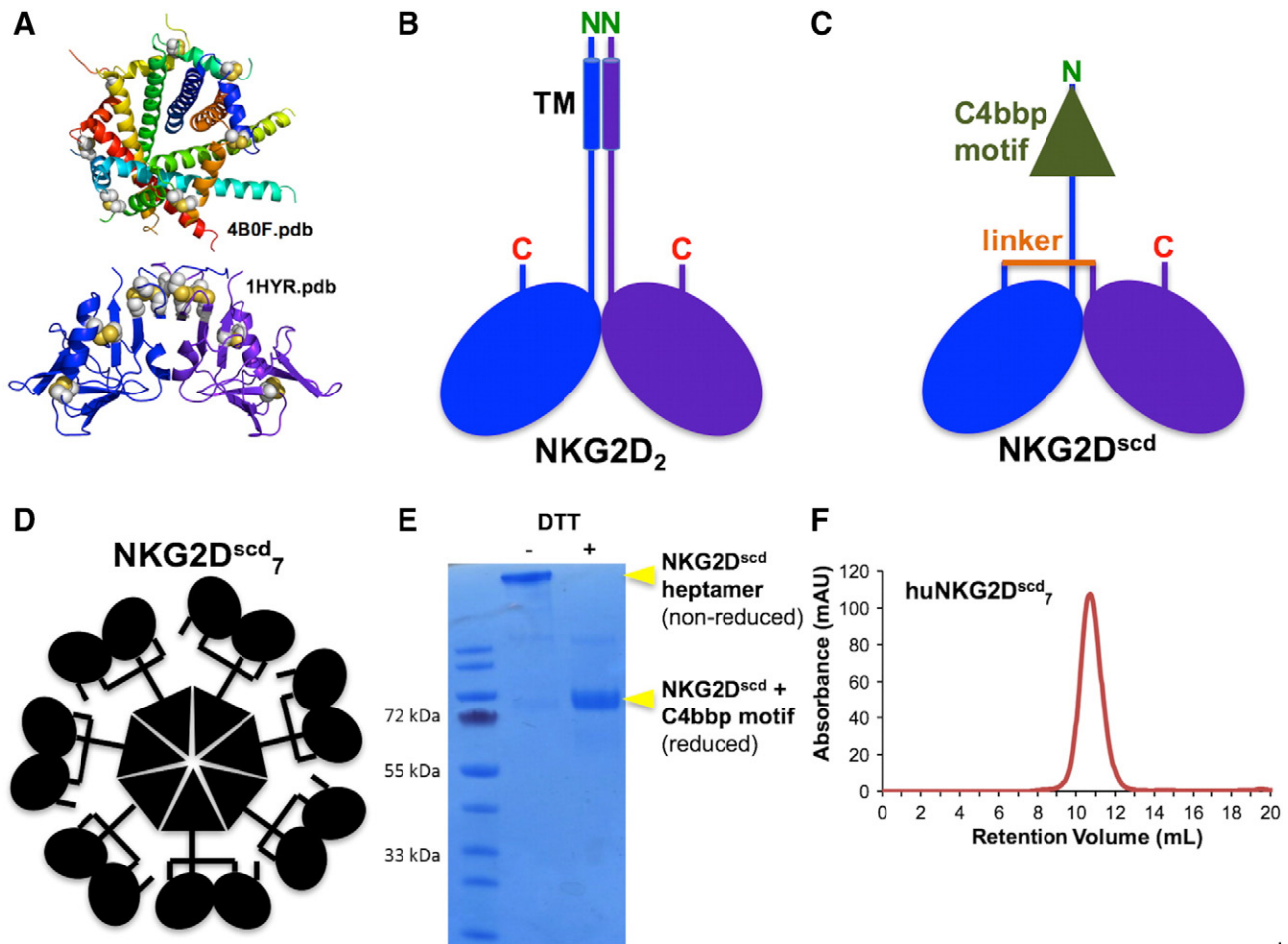


Figure 5. Engineering and properties of soluble NKG2D multimer. (A) Ribbon representations of the crystal structures (colored by chain) of the C4bbp heptamerization motif (top) and the NKG2D homodimeric ectodomain recognition unit (bottom). Disulfide bonds are shown as gray-and-yellow spheres. (B and C) Schematic representations of the native NKG2D homodimer and the NKG2D^{scd}₇ protomer, detailing key features. (D) Schematic representation of the overall molecular arrangement of the NKG2D^{scd}₇ multimer. (E) Comparative reduced/nonreduced polyacrylamide gel electrophoresis analysis confirming purity and disulfide bond formation. (F) Analytical SEC showing solution monodispersivity of human NKG2D^{scd}₇ multimer.

tumor-initiating capacity of NKG2D⁺ ovarian cancer cells (Figure 6C). To assess the relative contribution of NKG2D to overall tumor initiation capacity, NSG mice were engrafted with unsorted EOC cells and NKG2D stimulation disabled by NKG2D RNAi transduction or NKG2D^{scd}₇-mediated ligand masking. Unlike the controls, none of the experimental implants generated tumors, suggesting a prominent role of NKG2D and its ligands in EOC tumorigenicity (Figure 6D).

Discussion

Expression of cell surface receptors encoded in the human NK gene complex is typically restricted to cells of hematopoietic origin. An

apparent exception is NKG2D, which, in addition to its normal distribution on CD8 T cells and NK cells, is also found on different types of cancer cells [4]. Previous *in vitro* studies and correlative observations in *ex vivo* cancer specimens have provided tentative evidence for a role of cancer cell NKG2D in the epithelial to mesenchymal transition, but its full oncogenic potential as an inducer of stemness has remained unknown [17]. We now show that NKG2D⁺ ovarian cancer cells have the capacity for self-renewing sphere formation and efficient tumor initiation upon implantation into immunodeficient mice. Moreover, we provide formal evidence that ligand triggering of NKG2D underlies this functional capacity.

Figure 4. NKG2D stimulates stem cell-like functional capacities in a transfected human tumor line. (A) Phase contrast micrographs of tumor spheres formed by MDAH-2774-TF, parental MDAH-2774, and MDAH-2774-TF-KO cells, each plated at 1×10^3 cells/well. (B) Bar graph at left displays average numbers of spheres (>100 μm) counted in three sets of triplicate wells seeded with the indicated cells. Bar graph at right represents average numbers of spheres formed by MDAH-2774-TF cells in the presence of anti-NKG2DL Abs or isotype Ig. Data from both graphs are representative of three independent experiments. (C) Tumor initiation capacities of MDAH-2774-TF, MDAH-2774, MDAH-2774 mock, and MDAH-2774-TF-KO cells implanted subcutaneously into flanks of NOD/SCID mice at the cell numbers indicated. Numbers in top horizontal line indicate weeks post tumor cell inoculation. Left vertical columns list mouse identification (ID) numbers. Dark and light gray boxes indicate presence and absence of measurable tumors, respectively. White fields indicate that animals were euthanized due to tumor size. (D) Xenograft tumor incidence expressed as numbers of tumors formed per numbers of inoculations of 100 or 1000 MDAH-2774-TF cells into NOD/SCID mice treated with anti-NKG2DL Abs or control Ig either locally at cell inoculation site or *via* tail vein injection.

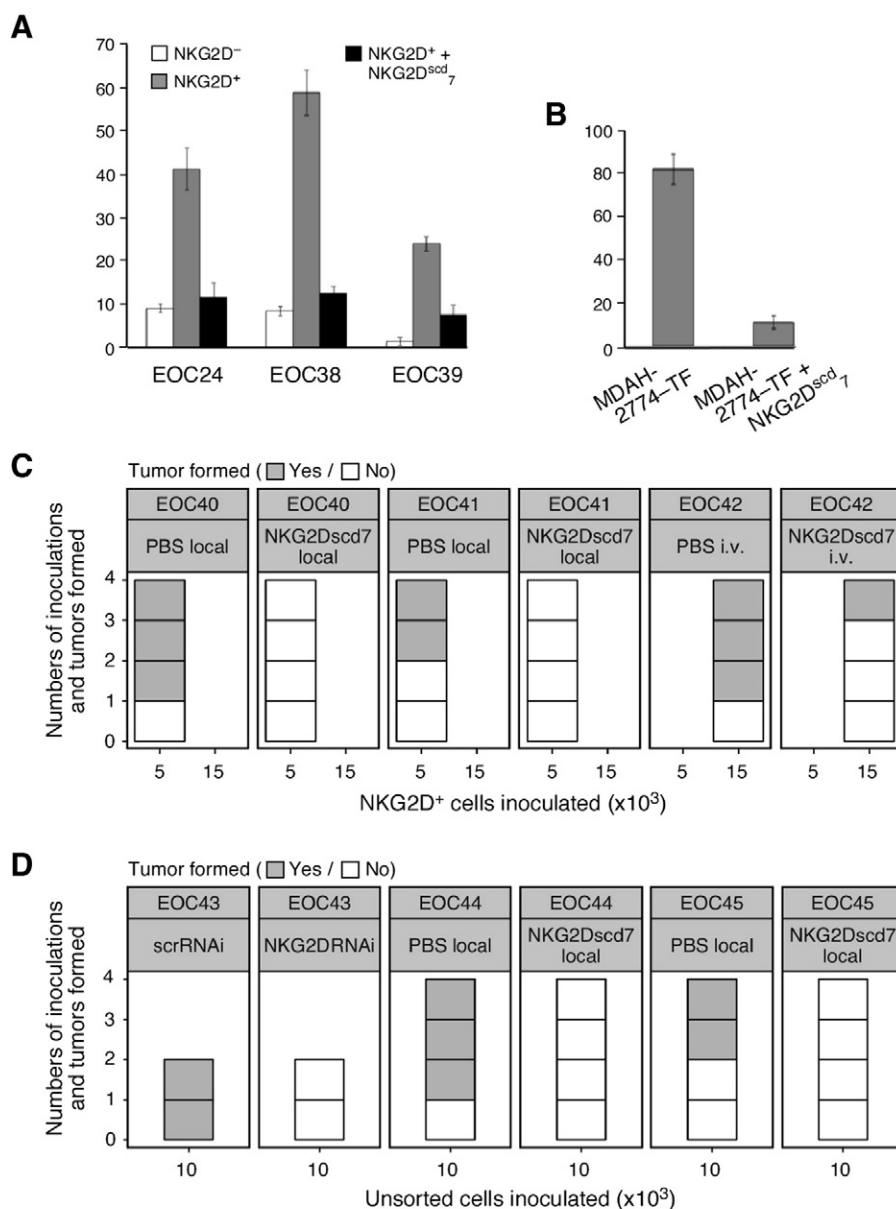


Figure 6. Involvement of NKG2DL in cancer cell NKG2D-driven sphere formation and tumor initiation. (A) Display of average numbers (derived from triplicate wells seeded with 5×10^3 cells) of spheres ($>100 \mu\text{m}$) formed by NKG2D⁺ HGS EOC cells in the presence (black bars) or absence (gray bars) of NKG2D^{scd7}. Open bars represent average numbers of spheres formed by matching NKG2D⁻ cancer cells. (B) Average numbers (derived from triplicate wells seeded with 1×10^3 cells) of spheres ($>100 \mu\text{m}$) formed by MDAH-2774-TF cells in the presence or absence of NKG2D^{scd7}. Data are representative of three independent experiments. (C) Xenograft tumor incidence expressed as numbers of tumors formed per number of inoculations of NKG2D⁺ cancer cells into NSG mice treated locally or systemically with NKG2D^{scd7} or control PBS. EOC40 and EOC41 represent HGS EOC; EOC42 represents type I ovarian cancer. Numbers of cells inoculated are indicated on X-axis and were guided by specimen size. (D) Xenograft tumor incidence expressed as numbers of tumors formed per number of inoculations of *ex vivo* isolated unsorted cancer cells into NSG mice. EOC43-derived cells were transduced with NKG2D RNAi or control scrRNAi; mice inoculated with EOC44 or EOC45 cells received subcutaneous NKG2D^{scd7} or control PBS. EOC43 and EOC45 are HGS EOC; EOC44 represents type I ovarian cancer.

Our results further suggest that NKG2D-driven tumor initiation accounts for a significant proportion of the overall tumor initiation potential of a given ovarian cancer. NKG2D and its ligands may thus represent an important regulator of tumorigenesis and dissemination, offering an explanation for the negative clinical associations found between frequencies of NKG2D⁺ or NKG2DL⁺ cancer cells and disease outcome (see Figure 1 [11–15]). In all likelihood, a tumor-initiating role of NKG2D also applies to malignancies other

than ovarian cancer studied here, such as breast, colon, prostate, and certain liquid cancers harboring NKG2D⁺ cancer cells [4,38,39].

The intratumoral localization and *in situ* context of cancer cells expressing functional surface NKG2D remain unknown because immunohistology in tissue sections is unsuitable for unequivocally distinguishing between surface and intracellular protein. Our earlier study noted that within any given tumor, proportions of cancer cells scoring positive by immunohistochemistry exceeded those

simultaneously recorded by surface flow cytometry, most likely reflecting the presence of cancer cells with intracellular but no surface NKG2D [4]. With no evidence for endosomal signaling, these discrepancies imply the presence of NKG2D⁺ cancer cells that lack functional surface expression and thus NKG2D-related biological significance [4]. Similarly unknown are factors controlling the nonlymphocyte expression of NKG2D-DAP10. However, there is precedent for cancers breaching control of cell-type specificity of certain cell surface receptors [40]. For example, cancer-associated abundance of vascular endothelial growth factor is complemented by cancer cell expression of the normally endothelial vascular endothelial growth factor receptor 2 [41]. Similarly, certain chemokines or cytokines in tumor microenvironments lead to atypical chemokine and cytokine receptor expression on cancer cells [42].

NKG2D and its ligands are recognized as modulators of tumor immunity and as such of interest to cancer immunotherapy [43–46]. Among current approaches are the development of multivalent immunoligands containing MICA or ULBP2 for stimulation of T cell and NK cell NKG2D [47–49] and pharmacological enhancement of NKG2D ligand expression [50]. Without selectivity for lymphocyte NKG2D, however, such efforts may have unwanted consequences due to simultaneous augmentation of cancer cell NKG2D signaling and its effects on tumor initiation. In light of our clinical association data, however, blocking cancer cell NKG2D through ligand masking might be beneficial regardless of simultaneous inhibitory effects on lymphocyte NKG2D [2]. Thus, the pan-NKG2DL–masking NKG2D^{scd}₇ reagent employed in this study may represent a promising tool for further investigation. However, larger-scale assessments of the relative contributions of cancer cell and/or lymphocyte NKG2D to tumor promotion would be desirable to further inform NKG2D-based tumor immunotherapy approaches. As with the current study, such efforts would have to record the biologically relevant cell surface NKG2D protein. Interrogation of cancer gene expression databases would not provide the desired insight because it would allow neither the distinction of cancer cell and lymphocyte NKG2D nor the assessment of cell surface protein.

In conclusion, our study identifies a new mechanism whereby cancers abuse an immune receptor ligand axis normally employed for protection against transformed cells for the induction of cancer stem cell–like tumor initiation in ovarian cancer and possibly other malignancies. We show that this tumor-promoting role of NKG2D has significant clinical consequences, thus presumably representing the main factor underlying the typically poor clinical outcomes that have been associated with expression of NKG2DL in ovarian and other cancers [11–15].

Acknowledgements

We thank Dr. Martin Prlic for technical advice and discussions; Della Friend for SPR analyses; and Kathy O'Briant, Erika Tone, and Shirley Gough of the Pacific Ovarian Cancer Research Consortium, and the CHTN Western Division for tumor tissue procurement.

Appendix A. Supplementary data

Supplementary data to this article can be found online at <http://dx.doi.org/10.1016/j.neo.2017.03.005>.

References

- Ullrich E, Koch J, Cerwenka A, and Steinle A (2013). New prospects on the NKG2D/NKG2DL system for oncology. *Oncoimmunology* **2**(10), e26097.
- Groh V, Wu J, Yee C, and Spies T (2002). Tumour-derived soluble MIC ligands impair expression of NKG2D and T-cell activation. *Nature* **419**(6908), 734–738.
- Hanaoka N, Jabri B, Dai Z, Ciszewski C, Stevens AM, Yee C, Nakahuma H, Spies T, and Groh V (2010). NKG2D initiates caspase-mediated CD3zeta degradation and lymphocyte receptor impairments associated with human cancer and autoimmune disease. *J Immunol* **185**(10), 5732–5742.
- Benitez AC, Dai Z, Mann HH, Reeves RS, Margineantu DH, Gooley TA, Groh V, and Spies T (2011). Expression, signaling proficiency, and stimulatory function of the NKG2D lymphocyte receptor in human cancer cells. *Proc Natl Acad Sci U S A* **108**(10), 4081–4086.
- Upshaw JL and Leibson PJ (2006). NKG2D-mediated activation of cytotoxic lymphocytes: unique signaling pathways and distinct functional outcomes. *Semin Immunol* **18**(3), 167–175.
- Vivanco I and Sawyers CL (2002). The phosphatidylinositol 3-kinase AKT pathway in human cancer. *Nat Rev Cancer* **2**(7), 489–501.
- Normanno N, De Luca A, Bianco C, Strizzi L, Mancino M, Maiello MR, Carotenuto A, De Feo G, Caponigro F, and Salomon DS (2006). Epidermal growth factor receptor (EGFR) signaling in cancer. *Gene* **366**(1), 2–16.
- Eagle RA and Trowsdale J (2007). Promiscuity and the single receptor: NKG2D. *Nat Rev Immunol* **7**(9), 737–744.
- Raulat DH, Gasser S, Gowen BG, Deng W, and Jung H (2013). Regulation of ligands for the NKG2D activating receptor. *Annu Rev Immunol* **31**, 413–441.
- Groh V, Rhinehart R, Secrist H, Bauer S, Grabstein KH, and Spies T (1999). Broad tumor-associated expression and recognition by tumor-derived gamma delta T cells of MICA and MICB. *Proc Natl Acad Sci U S A* **96**(12), 6879–6884.
- McGilvray RW, Eagle RA, Rolland P, Jafferji I, Trowsdale J, and Durrant LG (2010). ULBP2 and RAET1E NKG2D ligands are independent predictors of poor prognosis in ovarian cancer patients. *Int J Cancer* **127**(6), 1412–1420.
- Wu JD, Higgins LM, Steinle A, Cosman D, Haugk K, and Plymate SR (2004). Prevalent expression of the immunostimulatory MHC class I chain-related molecule is counteracted by shedding in prostate cancer. *J Clin Invest* **114**(4), 560–568.
- Li K, Mandai M, Hamanishi J, Matsumura N, Suzuki A, Yagi H, Yamaguchi K, Baba T, Fujii S, and Knosi I (2009). Clinical significance of the NKG2D ligands, MICA/B and ULBP2 in ovarian cancer: high expression of ULBP2 is an indicator of poor prognosis. *Cancer Immunol Immunother* **58**(5), 641–652.
- Duan X, Deng L, Chen X, Lu Y, Zhang Q, Zhang K, Hu Y, Zeng J, and Sun W (2011). Clinical significance of the immunostimulatory MHC class I chain-related molecule A and NKG2D receptor on NK cells in pancreatic cancer. *Med Oncol* **28**(2), 466–474.
- Fang L, Gong J, Wang Y, Liu R, Li Z, Wang Z, Zhang Y, Zhang Z, Song Z, and Yang A, et al (2014). MICA/B expression is inhibited by unfolded protein response and associated with poor prognosis in human hepatocellular carcinoma. *J Exp Clin Cancer Res* **33**, 76.
- Scheel C and Weinberg RA (2012). Cancer stem cells and epithelial-mesenchymal transition: concepts and molecular links. *Semin Cancer Biol* **22**(5–6), 396–403.
- Cai X, Dai Z, Reeves RS, Caballero-Benitez A, Duran KL, Delrow JJ, Porter PL, Spies T, and Groh V (2014). Autonomous stimulation of cancer cell plasticity by the human NKG2D lymphocyte receptor coexpressed with its ligands on cancer cells. *PLoS One* **9**(10), e108942.
- Robertson MJ, Cochran KJ, Cameron C, Le JM, Tantravahi R, and Ritz J (1996). Characterization of a cell line, NKL, derived from an aggressive human natural killer cell leukemia. *Exp Hematol* **24**(3), 406–415.
- Kurman RJ and Shih le M (2016). The dualistic model of ovarian carcinogenesis: revisited, revised, and expanded. *Am J Pathol* **186**(4), 733–747.
- Groh V, Smythe K, Dai Z, and Spies T (2006). Fas-ligand-mediated paracrine T cell regulation by the receptor NKG2D in tumor immunity. *Nat Immunol* **7**(7), 755–762.
- Hofmeyer T, Schmelz S, Degiacomi MT, Dal Peraro M, Daneschdar M, Scrima A, van den Heuvel J, Heinz DW, and Kolmar H (2013). Arranged sevenfold: structural insights into the C-terminal oligomerization domain of human C4b-binding protein. *J Mol Biol* **425**(8), 1302–1317.
- Bandaranayake AD, Correnti C, Ryu BY, Brault M, Strong RK, and Rawlings DJ (2011). Daedalus: a robust, turnkey platform for rapid production of decigram quantities of active recombinant proteins in human cell lines using novel lentiviral vectors. *Nucleic Acids Res* **39**(21), e143.

- [23] Finton KA, Larimore K, Larman HB, Friend D, Correnti C, Rupert PB, Elledge SJ, Greenberg PD, and Strong RK (2013). Autoreactivity and exceptional CDR plasticity (but not unusual polyspecificity) hinder elicitation of the anti-HIV antibody 4E10. *PLoS Pathog* **9**(9), e1003639.
- [24] Kim Y, Bigelow L, Borovilos M, Dementieva I, Duggan E, Eschenfeldt W, Hatzos C, Joachimiak G, Li H, and Maltseva N, et al (2008). Chapter 3. High-throughput protein purification for x-ray crystallography and NMR. *Adv Protein Chem Struct Biol* **75**, 85–105.
- [25] Li P, Morris DL, Willcox BE, Steinle A, Spies T, and Strong RK (2001). Complex structure of the activating immunoreceptor NKG2D and its MHC class I-like ligand MICA. *Nat Immunol* **2**(5), 443–451.
- [26] Kwong KY, Baskar S, Zhang H, Mackall CL, and Rader C (2008). Generation, affinity maturation, and characterization of a human anti-human NKG2D monoclonal antibody with dual antagonistic and agonistic activity. *J Mol Biol* **384**(5), 1143–1156.
- [27] Munz M, Baeuerle PA, and Gires O (2009). The emerging role of EpCAM in cancer and stem cell signaling. *Cancer Res* **69**(14), 5627–5629.
- [28] R Core team (2006). R: A Language and Environment for Statistical Computing. Vienna, Austria: R Foundation for Statistical Computing; 2006 [URL <https://www.R-project.org/>].
- [29] Hu Y and Smyth GK (2009). ELDA: extreme limiting dilution analysis for comparing depleted and enriched populations in stem cell and other assays. *J Immunol Methods* **347**(1–2), 70–78.
- [30] Silva IA, Bai S, McLean K, Yang K, Griffith K, Thomas D, Ginestier C, Johnston C, Kueck A, and Reynolds RK, et al (2011). Aldehyde dehydrogenase in combination with CD133 defines angiogenic ovarian cancer stem cells that portend poor patient survival. *Cancer Res* **71**(11), 3991–4001.
- [31] Strauss R, Li ZY, Liu Y, Beyer I, Persson J, Sova P, Möller T, Pesonen S, Hemminki A, and Hamerlik P, et al (2011). Analysis of epithelial and mesenchymal markers in ovarian cancer reveals phenotypic heterogeneity and plasticity. *PLoS One* **6**(1), e16186.
- [32] Kuroda T, Hirohashi Y, Torigoe T, Yasuda K, Takahashi A, Asanuma H, Morita R, Mariya T, Asano T, and Mizuuchi M, et al (2013). ALDH1-high ovarian cancer stem-like cells can be isolated from serous and clear cell adenocarcinoma cells, and ALDH1 high expression is associated with poor prognosis. *PLoS One* **8**(6), e65158.
- [33] Dontu G, Abdallah WM, Foley JM, Jackson KW, Clarke MF, Kawamura MJ, and Wicha MS (2003). In vitro propagation and transcriptional profiling of human mammary stem/progenitor cells. *Genes Dev* **17**(10), 1253–1270.
- [34] Liao J, Qian F, Tchabo N, Mhaweche-Fauceglia P, Beck A, Qian Z, Wang X, Huss WJ, Lele SB, and Morrison CD, et al (2014). Ovarian cancer spheroid cells with stem cell-like properties contribute to tumor generation, metastasis and chemotherapy resistance through hypoxia-resistant metabolism. *PLoS One* **9**(1), e84941.
- [35] Wang H, Paczulla A, and Lengerke C (2015). Evaluation of stem cell properties in human ovarian carcinoma cells using multi and single cell-based spheres assays. *J Vis Exp* **95**, e52259.
- [36] Ponti D, Costa A, Zaffaroni N, Pratesi G, Petrangolini G, Coradini D, Pilotti S, Pierotti MA, and Daidone MG (2005). Isolation and in vitro propagation of tumorigenic breast cancer cells with stem/progenitor cell properties. *Cancer Res* **65**(13), 5506–5511.
- [37] Kim GG, Donnenberg VS, Donnenberg AD, Gooding W, and Whiteside TL (2007). A novel multiparametric flow cytometry-based cytotoxicity assay simultaneously immunophenotypes effector cells: comparisons to a 4 h ⁵¹Cr-release assay. *J Immunol Methods* **325**(1–2), 51–66.
- [38] Guilloton F, de Thonel A, Jean C, Demur C, Mansat-De Mas V, Laurent G, and Quillet-Mary A (2005). TNF α stimulates NKG2D-mediated lytic activity of acute myeloid leukemic cells. *Leukemia* **19**(12), 2206–2214.
- [39] Tang M, Acheampong DO, Wang Y, Xie W, Wang M, and Zhang J (2016). Tumoral NKG2D alters cell cycle of acute myeloid leukemic cells and reduces NK cell-mediated immune surveillance. *Immunol Res* **64**(3), 754–764.
- [40] Tarin D (2012). Inappropriate gene expression in human cancer and its far-reaching biological and clinical significance. *Cancer Metastasis Rev* **31**(1–2), 21–39.
- [41] Hamerlik P, Lathia JD, Rasmussen R, Wu Q, Bartkova J, Lee M, Moudry P, Bartek Jr J, Fischer W, and Lukas J, et al (2012). Autocrine VEGF-VEGFR2-neuropilin-1 signaling promotes glioma stem-like cell viability and tumor growth. *J Exp Med* **209**(3), 507–520.
- [42] Coussens LM and Werb Z (2002). Inflammation and cancer. *Nature* **420**(6917), 860–867.
- [43] Spear P, Wu MR, Sentman ML, and Sentman CL (2013). NKG2D ligands as therapeutic targets. *Cancer Immun* **13**, 8–21.
- [44] Vyas M, Koehl U, Hallek M, and von Strandmann E (2014). Natural ligands and antibody-based fusion proteins: harnessing the immune system against cancer. *Trends Mol Med* **20**(2), 72–78.
- [45] Smits NC, Coupet TA, Godbersen C, and Sentman CL (2016). Designing multivalent proteins based on natural killer cell receptors and their ligands as immunotherapy for cancer. *Expert Opin Biol Ther* **16**(9), 1105–1112.
- [46] Wu J (2016). Antibody targeting soluble NKG2D ligand sMIC refuels and invigorates the endogenous immune system to fight cancer. *Oncoimmunology* **5**(3), e1095434.
- [47] Rothe A, Jachimowicz RD, Borchmann S, Madlener M, Kessler J, Reiners KS, Sauer M, Hansen HP, Ullrich RT, and Chatterjee S, et al (2014). The bispecific immunoligand ULBP2-aCEA redirects natural killer cells to tumor cells and reveals potent anti-tumor activity against colon carcinoma. *Int J Cancer* **134**(12), 2829–2840.
- [48] Wang T, Sun F, Xie W, Tang M, He H, Jia X, Tian X, Wang M, and Zhang J (2016). A bispecific protein rG7S-MICA recruits natural killer cells and enhances NKG2D-mediated immunosurveillance against hepatocellular carcinoma. *Cancer Lett* **372**(2), 166–178.
- [49] Xie W, Liu F, Wang Y, Ren X, Wang T, Chen Z, Tang M, Sun F, Li Z, and Wang M, et al (2016). VEGFR2 targeted antibody fused with MICA stimulates NKG2D mediated immunosurveillance and exhibits potent anti-tumor activity against breast cancer. *Oncotarget* **7**(13), 16445–16461.
- [50] Krieg S and Ullrich E (2012). Novel immune modulators used in hematology: impact on NK cells. *Front Immunol* **3**, 388.